



Review of CVD Synthetic Diamonds  
Reversible Color Alteration of Blue Zircon  
Sapphires from the Russian Far East  
Grandidierite from Madagascar

# SAPPHIRES FROM THE SUTARA PLACER IN THE RUSSIAN FAR EAST

Svetlana Yuryevna Buravleva, Sergey Zakharovich Smirnov, Vera Alekseevna Pakhomova, and Dmitrii Gennadyevich Fedoseev

From 2009 to 2011, sapphire crystals and corundum-bearing rocks were discovered at Sutara, in the Jewish Autonomous Region of the Russian Far East. These sapphires are typically translucent to semitransparent and blue to pinkish blue. Most of the crystals are heavily included and display prominent growth zoning, twinning planes, and abundant exsolution lamellae. Their primary fluid inclusions contain diaspore crystals and a low-density CO<sub>2</sub>-CH<sub>4</sub> mixture. These inclusions indicate that sapphire mineralization occurred by means of low-density aqueous-carbonic fluids, which were able to carry significant concentrations of alumina. These fluids may have formed as a result of thermal impact of granitic magma on carbonate country rocks. The authors consider Sutara a metamorphic occurrence that formed as a result of diffusive and metasomatic processes at a region of contact between carbonate rocks and pegmatite veins.

Sapphire deposits are widespread throughout Southeast Asia and Africa (Peretti et al., 2008; Schwarz et al., 2008; Shor and Weldon, 2009; Khoi et al., 2011; Dharmaratne et al., 2012). Russia's only placer deposit of gem-quality sapphire is at Nezametnoya (Pakhomova et al., 2006). Another Russian source of sapphire (figure 1) lies along the Sutara River, in the Jewish Autonomous Region bordering China (figure 2). The earliest discovery of corundum there came about as a result of gold mining (Shaposhnikov, 1945). In 1943, geologists discovered gray and blue sapphire fragments in the alluvium of the Sutara

River, but they showed little interest because gold mining was more important at the time. Scientific studies of the sapphire's mineral associations, genesis, and gemological characteristics were not performed before the mine was closed in 2005.

From 2009 to 2011, the authors conducted fieldwork searching for gem-quality sapphire in the basin of the Sutara River. Corundum-bearing rock samples and sapphire crystals were discovered at the outer limits of the area (Pakhomova et al., 2009). Cabochon-grade sapphire from Sutara (figure 3) recently underwent gemological and mineralogical study at the Far East Geological Institute, Far Eastern Branch of the Russian Academy of Sciences (FEGI FEB RAS) in Vladivostok.

## GEOLOGY AND OCCURRENCE

The bedrock of the Sutara mining region consists of early Cambrian siltstones, sandstones, gneiss, marbles, marbled limestones, and crystal slates that

Figure 1. Sapphire fragments from Sutara ranging from 0.6 to 4.4 ct. Photo by Svetlana Buravleva.



See end of article for About the Authors and Acknowledgments.

GEMS & GEMOLOGY, Vol. 52, No. 3, pp. 252–264,  
<http://dx.doi.org/10.5741/GEMS.52.3.252>

© 2016 Gemological Institute of America



Figure 2. The Sutara mine district is located in the Jewish Autonomous Region (Russian Far East), approximately 36 km (22 miles) southeast of the town of Obluche and about 200 km (124 miles) west of the city of Birobidzhan. Source: [www.google.ru/maps](http://www.google.ru/maps).

interstratify with clay slates, carbonate, and graphitic rocks (figure 4). Intrusive rocks are present as biotite granites, biotite and tourmaline leucogranites, veins of granitic pegmatites, and aplites.

### In Brief

- Between 2009 and 2011, the authors discovered sapphire crystals and corundum-bearing rocks in the Russian Far East.
- Primary (syngenetic) inclusions in the corundum consisted of diaspore crystals and a CO<sub>2</sub>-CH<sub>4</sub> mixture.
- Low-density aqueous-carbonic fluids may have formed as a result of thermal impact of granitic magma on carbonate country rocks.

Early research by Shaposhnikov (1945) identified four sources of corundum in Sutara, two of which occur in carbonaceous rocks and in veins of intruding light-colored granites of a late Paleozoic complex. The others occur in terrigenous-carbonaceous rocks intruded by early Paleozoic granites.

Investigation of corundum mineralization (Shaposhnikov, 1945; Kovrizhnykh, 1993) showed that carbonate rocks contact with granites and pegmatites. Gray and light gray granites, medium- and

fine-grained, which are sometimes aplitic (figure 5), consist of microcline, microperthite, oligoclase, quartz, and biotite; muscovite is less common. Secondary minerals are zircon, apatite, magnetite, and titanite. Carbonate rocks in contact with granites became marble, and serpentinites developed in the exo-

Figure 3. These 14.07 and 14.52 ct sapphire cabochons are from Sutara, Russia. Photo by Svetlana Buravleva.



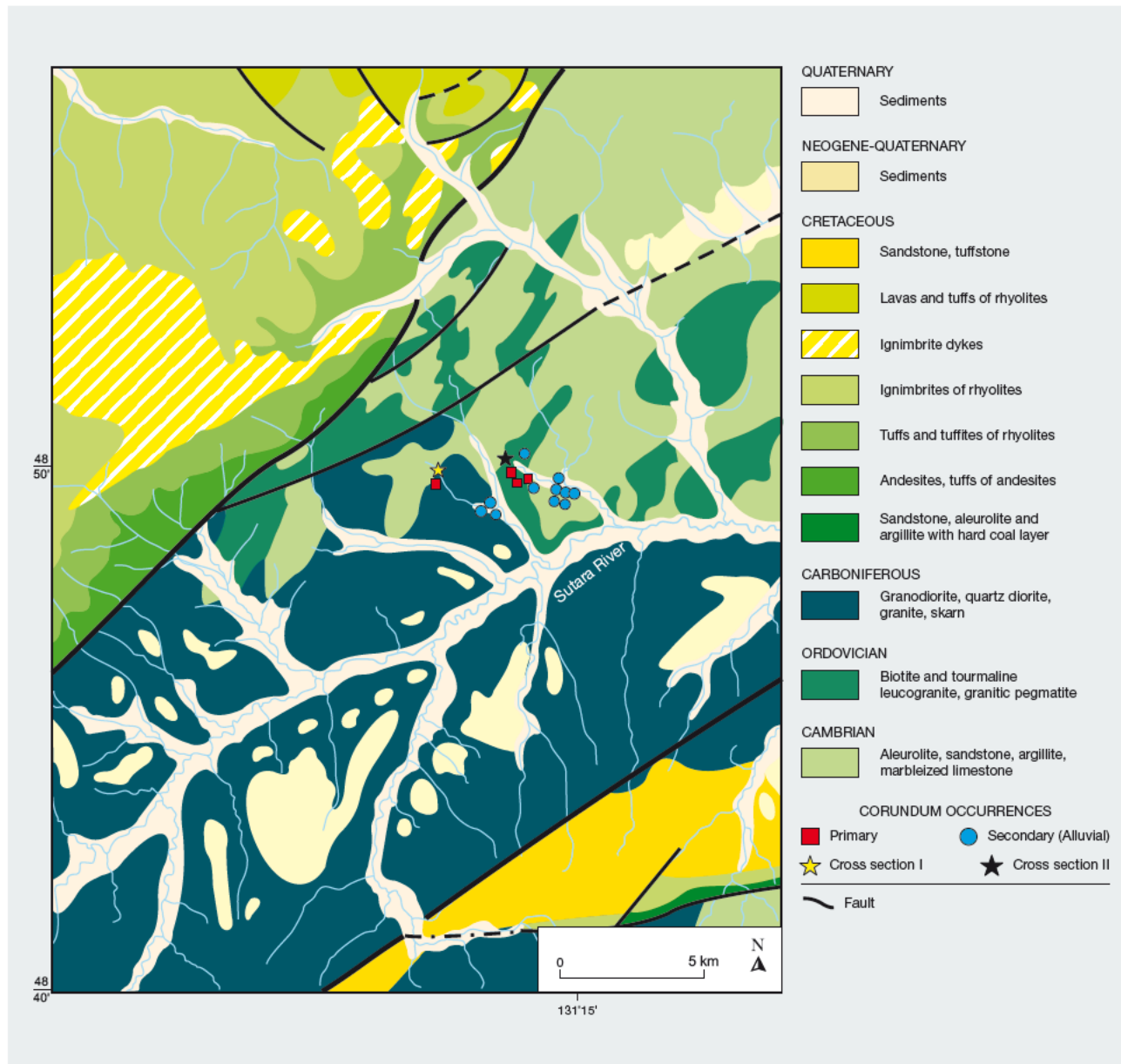


Figure 4. This simplified geologic map shows the primary and secondary (alluvial) sapphire occurrences discovered in the basin of the Sutara River. The basement is composed of metamorphosed carbonate rocks, intruded by granite and pegmatite. Adapted from Vaskin (1999).

contact zone. In the opicalcites, forsterite-bearing bodies are present. Similar associations are found as xenoliths in granites.

Opicalcites and serpentinites contain yellow forsterite, greenish phlogopite, tremolite, actinolite, and serpentine, sometimes creating ribboned structures. Secondary minerals of these rocks are calcite, talc, chlorite, and scapolite. Microscopic examina-

tion shows that the forsterite has been substantially converted to serpentine, which is present as fibrous chrysotile and needle-like antigorite.

Plagioclases (anorthosites) formed thin veins (from a few centimeters to a few meters thick) in the serpentinites, filling a transitional zone from granites to opicalcites. Plagioclases consist primarily of white plagioclase (anorthite) aggregates with minor

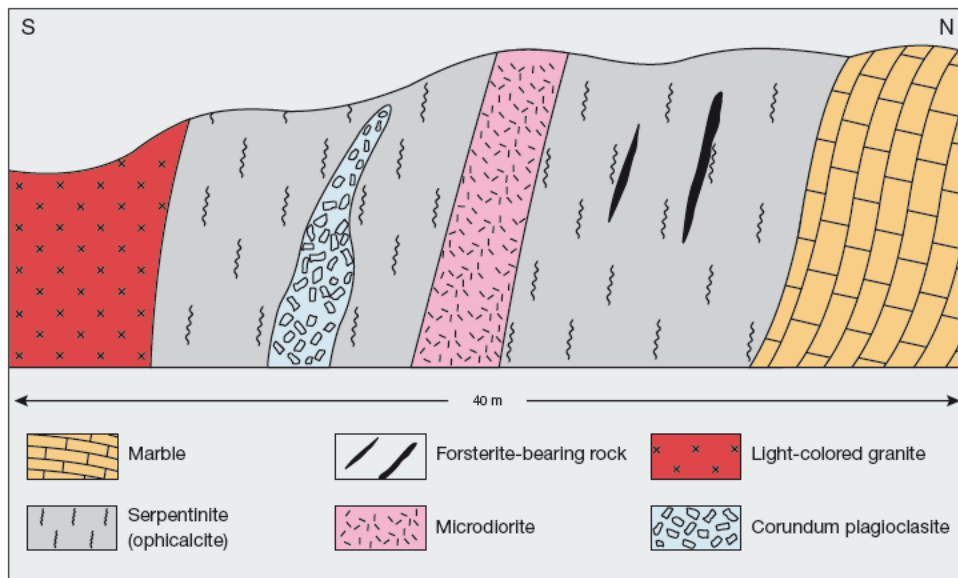


Figure 5. Schematic cross-section I. This illustration shows the primary corundum occurrence within the contact between light-colored granites and marbles. Corundum plagioclases consist of white plagioclase (anorthite), biotite, muscovite, and single sapphire crystals.

amounts of biotite and muscovite (about 5%). Sapphires occur as single translucent crystals of blue and pale purple color up to 1.5 cm in size, associated with plagioclase.

Bedrock exposures of corundum-bearing rocks (figure 6) were found in the Sutara district by Shaposhnikov in 1943. Here, two-mica granites break through quartz-micaceous slates with lenses of carbonate rocks. Within the contact of granites, a gradual transition from granites to pegmatites is observed. Carbonate rocks occur at a contact skarn that is defined by the presence of almandine (60%),

muscovite (30%), and epidote and chlorite (10%). In other sites outside the contact, the ophicalcites and serpentinites developed in a similar fashion.

On contact with carbonate rocks, pegmatites became desilicated and formed single well-formed bipyramidal crystals of corundum. Lenses ranging from 10 to 20 cm wide are visible, represented by near-monomineral varieties of corundum-bearing rocks with small amounts of margarite, vermiculite, and diaspre filling the interstices between the corundum crystals (figure 7).

The secondary (alluvial) sapphire occurrence was

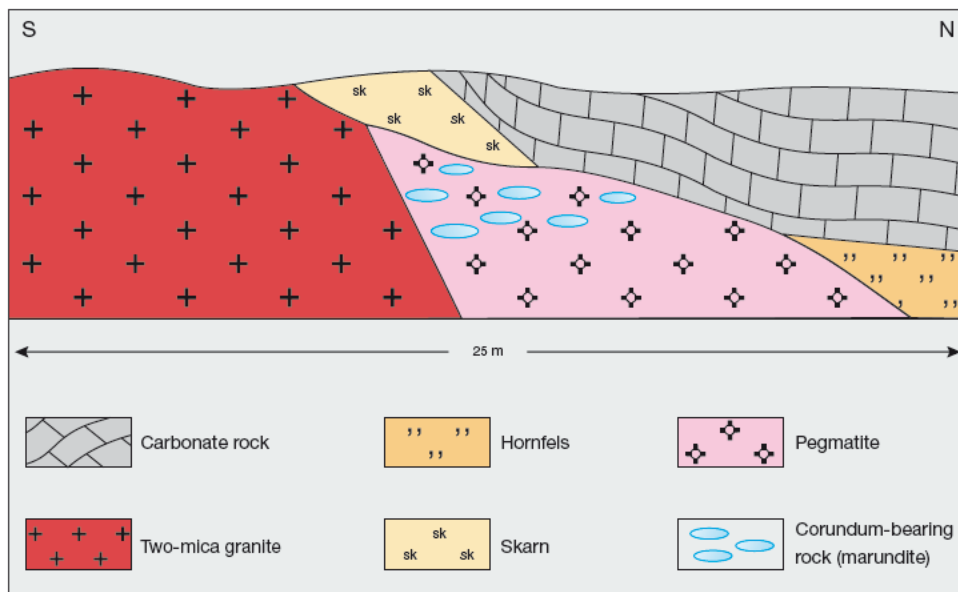


Figure 6. Schematic cross-section II. This illustration shows the primary corundum occurrence at the contact zone of pegmatite and carbonate rocks. Lenses of corundum-bearing rocks consist of brittle mica (margarite) between the corundum crystals.



Figure 7. This corundum-bearing rock sample from Sutara (2.8 × 2.0 cm) contains 70–90% corundum; the remainder is mostly mica (margarite). Photo by Svetlana Buravleva.

discovered in the basin of the Sutara River. The alluvium consists of a sapphire- and garnet-bearing layer above the bedrock that contains sand, pebbles, and boulders.

#### MATERIALS AND METHODS

We examined 139 samples (primary and alluvial) collected during three visits to the Sutara mine between 2009 and 2011. These consisted of five cut sapphires (up to 65.5 ct; figures 8 and 17), 57 rough specimens (up to 33 ct), 34 windowed sapphires, 18 thin sections of corundum-bearing rocks, and 25 parallel plates of the corundum-bearing rocks cut and polished for spectroscopy.

Standard gemological testing was performed at the gemological laboratory of the FEGI FEB RAS. A refractometer was used to measure refractive index and birefringence. Fluorescence was observed with long- and short-wave UV lamps (365 and 254 nm, respectively) in a darkened room. We measured carat weights with Sartorius jewelry scales and determined specific gravity hydrostatically. Internal features were observed with a standard gemological microscope and a Nikon Eclipse LV100 POL polarizing microscope.

Inclusions in 17 samples were analyzed by Raman spectroscopy using a Horiba LabRAM HR 800 spectrometer coupled with a Si-based charge-coupled device (CCD) detector and a Melles Griot 514 nm Ar<sup>+</sup> green laser. These analyses were performed at the V.S. Sobolev Institute of Geology and Mineralogy, Siberian Branch of the Russian Academy of Sciences (IGM SB RAS, Novosibirsk).

Quantitative chemical analyses on a total of 67 spots were carried out on seven parallel-plated sapphires and four corundum-bearing rocks using a JEOL JXA-8100 electron microprobe at the Primorye Shared Analytical Center for Local Elemental and Isotope Analysis in Vladivostok. Three wavelength-dispersive spectrometers with LIF, PET, TAP, and LDE2 crystal analyzers in the microprobe and an Inca energy-dispersive X-ray spectrometer were used. Analyses were performed under the following conditions: 20 kV accelerating voltage, 10 nA beam current, and 1 μm spot size. Detection limits for TiO<sub>2</sub> and Fe<sub>2</sub>O<sub>3</sub> were 0.05 wt. %.

Trace element chemical data of seven alluvial sapphires were measured quantitatively by inductively coupled plasma–mass spectrometry (ICP-MS) at the Primorye Center using an Agilent 7500c mass spectrometer. Laser ablation was not used. Samples were melted with lithium metaborate (LiBO<sub>2</sub>) on platinum melting pots. Detection limits were typically 0.01–0.05 parts per million by weight (ppmw) for the solid component. Calibration solutions for ICP-MS were prepared from multi-element certified solutions. For defined elements, the following isotopes were chosen: <sup>9</sup>Be, <sup>45</sup>Sc, <sup>51</sup>V, <sup>52</sup>Cr, <sup>59</sup>Co, <sup>60</sup>Ni, <sup>63</sup>Cu, <sup>66</sup>Zn, <sup>71</sup>Ga, <sup>85</sup>Rb, <sup>88</sup>Sr, <sup>89</sup>Y, <sup>90</sup>Zr, <sup>93</sup>Nb, <sup>118</sup>Sn, <sup>133</sup>Cs, <sup>139</sup>La, <sup>140</sup>Ce, <sup>141</sup>Pr, <sup>146</sup>Nd, <sup>181</sup>Ta, <sup>232</sup>Th, <sup>182</sup>W, and <sup>208</sup>Pb. The plasma conditions of the ICP-MS were optimized to an intensity of CeO/Ce 156/140 < 0.750% and Ce<sup>++</sup>/Ce<sup>+</sup> 70/140 < 2%. This was achieved using the following parameters: plasma gas flow (Ar) of 15.0 liters per

Figure 8. This 2.22 ct sapphire cabochon is one of the samples from Sutara. Photo by Svetlana Buravleva.





Figure 9. These Sutarra sapphire crystals show bipyramidal (four samples) and short prismatic (one sample) forms. The bipyramidal crystals are dominated by  $v$  faces with various combinations of  $c$ ,  $r$ ,  $s$ , and  $v$ ; they do not show  $a$  faces. The short prismatic forms consist of various combinations of  $c$ ,  $a$ ,  $r$ , and  $s$  faces (Schwarz et al., 2008). Photos by Svetlana Buravleva.

minute, nebulizer gas flow (Ar) of 1.14–1.19 liters per minute, and auxiliary gas flow (Ar) of 1.0 liter per minute. Sensitivity was tuned using Agilent tuning solution, containing 10 mg/l  $^{140}\text{Ce}$ ,  $^{59}\text{Co}$ ,  $^7\text{Li}$ ,  $^{205}\text{Tl}$ , and  $^{89}\text{Y}$ . The background signal was controlled by measuring the signal intensity of  $^{45}\text{Sc}$  in Agilent tuning solution, since scandium is absent in it. The intensity of the  $^{45}\text{Sc}$  signal was <70 counts per second, with an integration time of 0.1 seconds.

Elemental analyses of five alluvial sapphires were measured quantitatively by inductively coupled plasma–atomic emission spectroscopy (ICP–AES) at the Primorye Center using an iCAP 6500 Duo spectrometer. This instrument combines an Echelle optical spectrometer with a semiconductive CID detector and a system for radial and axial observations of a plasma charge. Detection limits in the solution were typically 0.01–0.07 ppm (Al = 0.07, Ti = 0.002, Fe = 0.005, Ca = 0.011, Mg = 0.012, Mn = 0.001, K = 0.031,

Na = 0.128, P = 0.053). For the determination of aluminum, we used a multivariate calibration solution of aluminum; to determine the remaining elements, we used Merck Certipur ICP multi-element standard solution IV as well as multi-element calibration standard-4. The material was carried to the ICP by Ar gas with the following parameters: plasma gas flow (Ar) of 12.0 liters per minute, nebulizer gas flow (Ar) of 0.6 liters per minute, auxiliary gas flow (Ar) of 0.5 liters per minute, and RF power of 1150 W. Sensitivity was again tuned using Agilent tuning solution.

### GEMOLOGICAL PROPERTIES

Alluvial sapphires from Sutarra are found as euhedral bipyramidal crystals or broken pieces, some weighing more than 65 ct. They display bipyramidal or short barrel habits, mainly with a combination of hexagonal prism  $a$  and basal pinacoid  $c$  faces (figure 9). Most bipyramidal crystal fragments showed  $v$  and

**TABLE 1.** Gemological characteristics of sapphires from Sutara, Russia.

Property	Gray sapphires from type 1 corundum-bearing rock	Blue sapphires from type 2 corundum-bearing rock	Alluvial sapphires
Color	Colorless, gray, bluish gray, and black	Colorless, blue, and bluish white	Blue, gray, bicolored pink and blue, violetish blue, and purplish pink
Color zoning	Irregular gray and white color patches	Irregular blue and white color patches	Strong color zoning is common. Some have patches of pink and blue colors.
Refractive Indices	$n_o = 1.768\text{--}1.770$ $n_e = 1.760\text{--}1.762$	$n_o = 1.767\text{--}1.770$ $n_e = 1.759\text{--}1.762$	$n_o = 1.768\text{--}1.770$ $n_e = 1.758\text{--}1.760$
Birefringence	0.008	0.008	0.010
Specific gravity	3.98–4.00	3.98–4.00	3.98–4.02
Optic character	Uniaxial negative	Uniaxial negative	Uniaxial negative
Fluorescence <sup>a</sup>	Inert to both LW and SW	Inert to both LW and SW	<i>Blue, gray, bicolored pink and blue, and violetish blue:</i> Inert to both LW and SW  <i>Purplish pink:</i> LW: Moderate to strong red SW: Inert to weak red
Internal features	<ul style="list-style-type: none"> <li>• Rutile needles, plagioclase, margarite, ilmenite, spinel, and pyrrhotite</li> <li>• Primary and secondary liquid-gas inclusions</li> <li>• Growth zoning, parting, fractures, and lamellar twinning</li> </ul>	<ul style="list-style-type: none"> <li>• Rutile needles, plagioclase, apatite, xenotime, muscovite, margarite, and boehmite</li> <li>• Primary and secondary liquid-gas inclusions</li> <li>• Growth zoning, parting, fractures, and lamellar twinning</li> </ul>	<ul style="list-style-type: none"> <li>• Rutile needles, zircon, biotite, monazite, xenotime, plagioclase, ilmenite, pyrite, and spinel</li> <li>• Primary and secondary liquid-gas inclusions</li> <li>• Growth zoning, parting, fractures, lamellar twinning, and trapiche stars</li> </ul>

<sup>a</sup>LW = long-wave ultraviolet radiation, SW = short-wave ultraviolet radiation

v faces. We observed *c* in combination with *r* and *s* faces. In the short prismatic crystals, basal pinacoid *c* and hexagonal prism *a* were dominant, with small *r* and *s* faces. Almost all of these crystals were characterized by polysynthetic twinning observed with a microscope. The colors observed ranged from blue, gray, bicolored pink and blue, violetish blue, yellowish, and purplish pink, varying in tone from very light to dark (again, see figure 1).

Some of the sapphires demonstrated strong dichroism. The samples' clarity ranged from semi-transparent to translucent and opaque. Their color pattern was often zoned and spotty (figure 10). Some of the gray samples showed silky patches and six-rayed trapiche-like patterns with oriented micro-inclusions, particularly rutile needles (figure 11).

The corundum-bearing rocks are classified here as type 1 and type 2 (table 1). Type 1 contains opaque gray, bluish gray, and black sapphire crystals; type 2

consists of blue and white zoned sapphire crystals (see figure 12). Both types are represented by almost monomineral varieties consisting of 70–90% sapphire crystals exhibiting a hexagonal prism shape.

**Mineral Inclusions.** The alluvial sapphires contained various mineral inclusions such as rutile, zircon, biotite, monazite, xenotime, plagioclase, ilmenite, pyrite, and spinel. Zircon, rutile, and biotite were the most common. These inclusions were identified by both Raman spectroscopy and electron microprobe analysis. Rutile usually occurred as short, dark three-dimensional networks of oriented needles (figure 13) or slightly brown irregular forms. Biotite occurred as single dark brown tabular crystals up to 70  $\mu\text{m}$  in size.

Zircon inclusions were transparent, well-developed prismatic crystals measuring up to 30  $\mu\text{m}$ , clustered in groups or compact agglomerations. Monazite occurred in irregular, slightly rounded forms up to 20



Figure 10. Multiple directions of growth zoning are often found in the Sutar sapphires. Photomicrograph by Svetlana Buravleva; transmitted light, field of view 1.10 mm.



Figure 11. This 7.2 ct sapphire with a trapiche-like pattern clearly displays the host's hexagonal symmetry (11.6 × 8.0 mm). Photo by Svetlana Buravleva.

µm in size. They were colorless, transparent, and associated with zircon crystals. Xenotime crystals up to 100 µm were transparent and nearly colorless, while others were slightly green. They were associated with zircon and monazite crystals (figure 14, left).

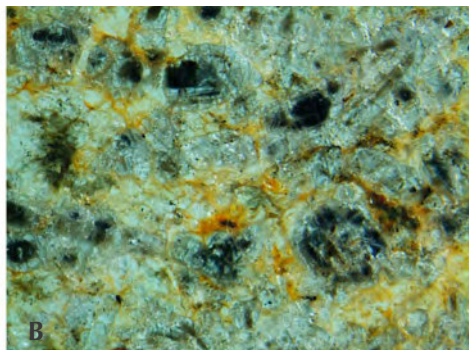
Plagioclase, identified by Raman spectrometry, was observed as well-developed transparent crystals

(figure 14, center). Electron microprobe analysis established that the plagioclase corresponded to andesine in composition.

Spinel was a rare mineral inclusion. Identified by electron microprobe as small Fe- and Mg-rich inclusions up to 10 µm in size, it was not visible during microscopic examination of the samples.



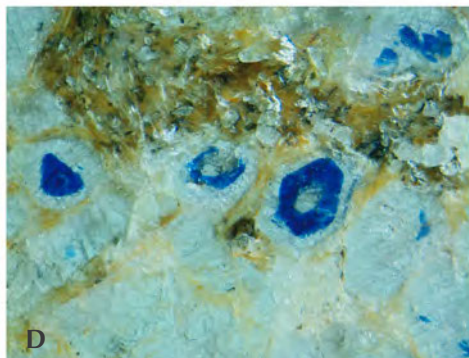
A



B



C



D

Figure 12. Corundum-bearing rocks, with mica filling the interstices between sapphire crystals, are represented by two types. Top: the first type 1 sample (left) and a parallel plate cut from it (right). Bottom: the second type 2 sample and the parallel plate cut from it. Photos and photomicrographs by Svetlana Buravleva; photomicrograph field of view 11 mm.



Figure 13. An example of oriented rutile needles in the Sutura sapphires. Photomicrograph by Svetlana Buravleva; field of view 0.55 mm.

In general, the primary and alluvial samples showed a similar range of mineral inclusions. Corundum from the primary occurrence also contained pyrrhotite (type 1), apatite, muscovite, and rarely boehmite (type 2).

**Fluid Inclusions.** Fluid inclusions in sapphires from primary and alluvial occurrences are similar. The study of syngenetic inclusions makes it possible to obtain accurate information on the conditions of mineral crystallization.

**TABLE 2.** Electron microprobe analyses (in wt.%) of two sapphires from the primary occurrence at Sutura, Russia.

Oxide	Type 1 <sup>a</sup>	Type 2 <sup>b</sup>
Al <sub>2</sub> O <sub>3</sub>	98.30 ± 0.16	98.78 ± 0.19
Fe <sub>2</sub> O <sub>3</sub>	0.65 ± 0.28	bdl <sup>c</sup>
TiO <sub>2</sub>	bdl	0.22 ± 0.04
<b>Total</b>	<b>98.95</b>	<b>99.00</b>

<sup>a</sup>Corundum-bearing rock with gray sapphires.

<sup>b</sup>Corundum-bearing rock with blue sapphires.

<sup>c</sup>bdl = below detection limit.

Detection limits for TiO<sub>2</sub> and Fe<sub>2</sub>O<sub>3</sub> are 0.05 wt. %.

Primary (syngenetic) inclusions (figure 14, right) were analyzed by Raman spectrometry. They consisted of diaspore, with a very strong peak at 448 cm<sup>-1</sup>; carbon dioxide, with peaks at 1284 and 1387 cm<sup>-1</sup>; and methane, with a 2914 cm<sup>-1</sup> peak (figure 15). The molecular ratios of carbon dioxide and methane were 0.989 and 0.011, respectively. Diaspore also occurs as the solid phase in three-phase inclusions, as in Sri Lankan sapphire (Schmetzer and Medenbach, 1988). Primary and secondary gas-liquid fluid inclusions were encountered frequently. Gas in the form of carbon dioxide showed peaks at 1284 and 1385 cm<sup>-1</sup>.

**Chemical Composition.** In sapphires from corundum-bearing rocks, electron microprobe analyses revealed concentrations of the chromophores Ti and Fe. Gray sapphires had an Fe<sub>2</sub>O<sub>3</sub> concentration of approximately 0.37–0.93 wt. % (table 2). Blue sapphires contained Fe<sub>2</sub>O<sub>3</sub> below the detection limit of 0.05 wt. %.

**TABLE 3.** Chemical composition by ICP-AES (in wt.%) of alluvial sapphires from Sutura, Russia.

Oxide	Pink			Blue		
	C-2	C-3	C-6	C-7	C-8	
Al <sub>2</sub> O <sub>3</sub>	98.65	91.10	97.30	98.25	91.15	
TiO <sub>2</sub>	0.09	0.08	0.09	0.07	0.10	
Fe <sub>2</sub> O <sub>3</sub>	1.15	1.31	1.14	1.09	1.22	
CaO	0.11	0.16	0.13	0.10	0.17	
MgO	0.09	0.13	0.11	0.09	0.14	
MnO	0.01	0.02	0.01	0.01	0.02	
K <sub>2</sub> O	0.46	0.62	0.54	0.43	0.66	
Na <sub>2</sub> O	0.36	0.51	0.42	0.36	0.56	
<b>Total</b>	<b>100.94</b>	<b>93.94</b>	<b>99.75</b>	<b>100.45</b>	<b>94.05</b>	

Note: Detection limits in the solution are typically 1 × 10<sup>-6</sup> to 7 × 10<sup>-6</sup> wt. % (0.01–0.07 ppm).

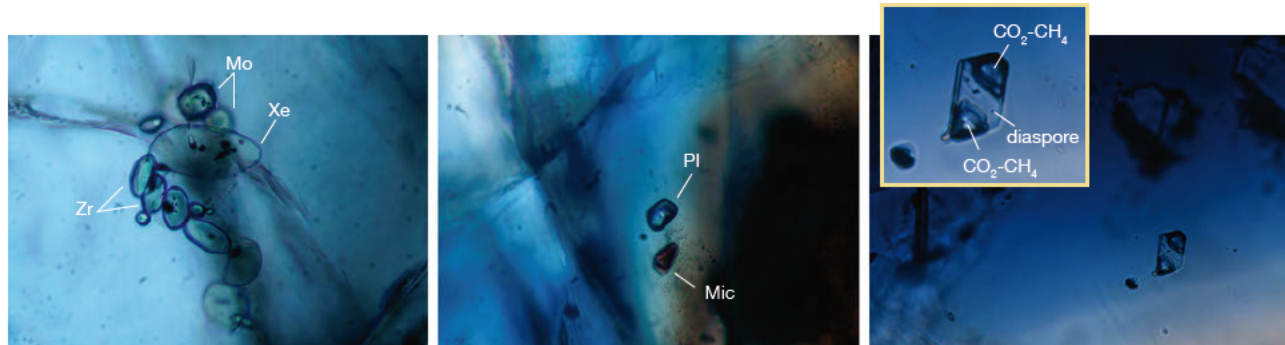


Figure 14. Left: Monazite (Mo), zircon (Zr), and xenotime (Xe) in the Sutura sapphires. Center: Transparent plagioclase (Pl) and mica (Mic) in the Sutura sapphires. Right: These primary fluid inclusions in sapphire contain diaspore crystals and a low-density CO<sub>2</sub>-CH<sub>4</sub> mixture. Photomicrographs by Svetlana Buravleva; field of view 0.22 mm.

In the blue sapphires, the TiO<sub>2</sub> concentration was approximately 0.11–0.26 wt.%. Type 1 gray sapphires

from the primary occurrence had TiO<sub>2</sub> below the detection limit.

TABLE 4. Trace element composition (in ppmw) of alluvial sapphire from Sutura, Russia, measured by ICP-MS.

Trace element	Pink			Gray		Blue	
	C-1	C-2	C-3	C-5	C-6	C-7	C-8
Be	0.28	0.12	0.08	0.60	0.06	0.07	0.10
Sc	2.40	0.99	1.96	1.62	1.92	1.42	1.99
V	36.49	37.71	61.58	34.99	32.37	36.85	42.30
Cr	203.50	202.10	260.90	209.90	181.90	201.20	220.60
Co	0.71	0.55	0.77	0.38	0.58	0.45	0.85
Ni	5.13	2.11	2.43	2.87	1.75	2.33	3.99
Cu	bdl						
Zn	16.10	18.73	13.95	34.94	16.90	10.08	8.60
Ga	69.09	74.57	93.47	75.69	76.57	73.52	75.32
Rb	7.78	5.64	8.23	5.84	4.75	5.44	8.20
Sr	9.42	8.47	10.65	8.15	11.81	8.11	11.49
Y	23.67	16.68	36.89	5.61	14.50	43.60	48.06
Zr	96.11	69.27	134.20	44.32	150.00	245.80	187.70
Nb	0.63	0.40	0.70	0.45	1.02	0.64	0.89
Sn	0.82	1.89	4.88	1.89	0.52	0.01	0.07
Cs	1.24	0.08	0.09	0.42	0.09	0.08	0.09
Ba	132.30	97.24	153.00	106.80	120.30	100.90	155.00
La	18.57	22.40	24.12	2.40	17.35	32.35	42.04
Ce	40.87	46.58	50.49	4.70	38.50	69.39	90.59
Pr	4.89	5.57	6.09	0.64	4.68	7.88	10.57
Nd	19.28	21.06	23.59	3.04	17.96	30.44	41.87
Ta	0.20	0.51	0.13	0.53	0.06	0.44	2.18
W	0.44	0.33	0.47	0.52	1.10	0.50	1.51
Pb	4.43	8.96	6.92	9.98	4.60	3.82	3.67
Th	6.28	7.77	8.07	1.22	7.86	13.57	13.89

Note: bdl = below detection limit. Detection limits are typically 0.01–0.05 ppmw for the solid component.

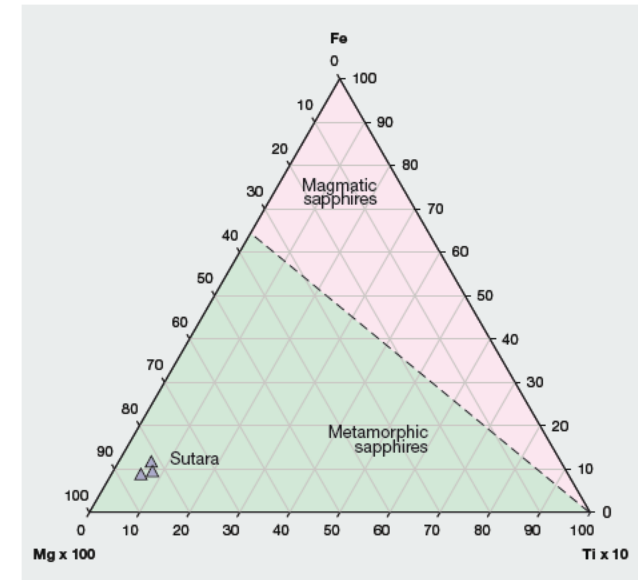
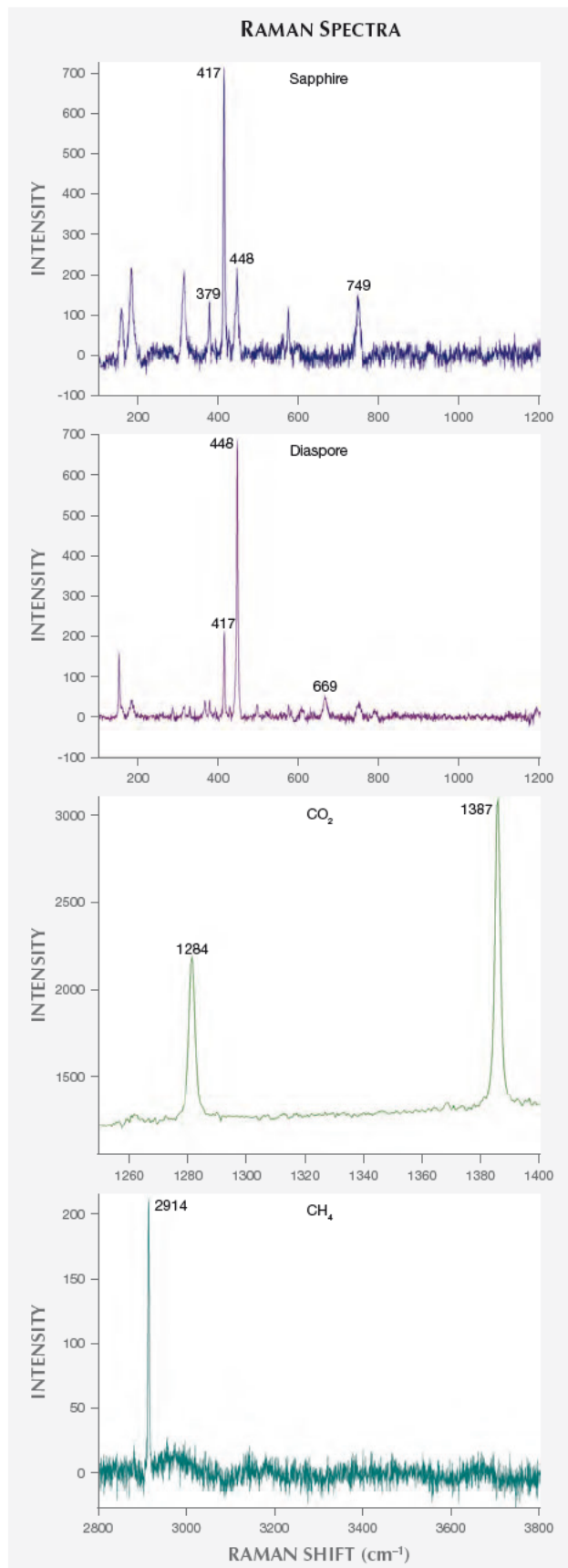


Figure 16. This ternary diagram shows the relative percentages of the elements Fe, Mg, and Ti (in ppmw) in blue alluvial sapphires from Sutarra. Modified from Peucat et al. (2007).

Both the pink and blue alluvial sapphires had a relatively high  $\text{Fe}_2\text{O}_3$  concentration, ranging from 1.09 to 1.31 wt. % (table 3). Their  $\text{TiO}_2$  concentration ranged from 0.07 to 0.10 wt. %.

ICP-MS data of trace elements in the alluvial sapphires are shown in table 4. Cr was abundant, with concentrations above 200 ppm (0.02 wt. %). The V concentration was generally low, from 32 to 61 ppm. Ga content ranged from 69 to 93 ppm. The detection limit was 0.01–0.05 ppm. Gray sapphire had the lowest concentrations of most trace elements.

Trace element chemical data of alluvial sapphires measured by ICP-MS revealed high concentrations, compared to sapphire in general, of Zr (44.32–245.80 ppmw), Cr (181.9–260.9 ppmw), Th (1.22–13.89 ppmw), La (2.40–42.04 ppmw), Ce (4.7–90.59 ppmw), Nd (3.04–41.87 ppmw), Y (5.61–48.06 ppmw), V

Figure 15. Raman spectra of the primary syngenetic inclusion in sapphire in figure 14, right. The sapphire host displayed a peak at  $417\text{ cm}^{-1}$ , while the primary inclusion consisted of a diaspore crystal with a peak at  $448\text{ cm}^{-1}$ , carbon dioxide ( $\text{CO}_2$ ) with peaks at  $1284$  and  $1387\text{ cm}^{-1}$ , and methane ( $\text{CH}_4$ ) with a peak at  $2914\text{ cm}^{-1}$ . Raman spectra were collected with a 514 nm laser.

(32.37–61.58 ppmw), and Pr (0.64–10.57 ppmw). Many of these trace elements might be the result of contamination by inclusions.

## DISCUSSION

Peucat et al. (2007) showed that differences in the composition of trace elements exist between magmatic and metamorphic corundum. He developed Fe-Mg-Ti diagrams, which also separate magmatic and metamorphic fields based on contrasting Fe/Mg ratios (figure 16). High Mg values are found in metamorphic sapphires only. Concentrations of Mg, Ti, and Fe (table 3) in the blue alluvial sapphires indicated metamorphic origin of Sutara corundum. Sapphires from Sutara plot in the metamorphic field. Their high Mg content is in agreement with the high Mg content of the carbonate rocks.

The geochemical characteristics of this corundum from Sutara are high total rare earth element (REE) contents and enrichment with Ba, Rb, and Sr compared to sapphires in general (Peretti et al., 2008). Thus, the main factor in the formation of this corundum mineralization is deep fluids enriched by Al, Ti, Zr, Ba, Sr, V, Cl, and REE.

Sapphires from the primary and alluvial occurrences at Sutara have similar inclusions. The syngenetic inclusions' composition can be determined using Raman spectrometry. These inclusions contain diaspore crystals and a low-density CO<sub>2</sub>-CH<sub>4</sub> mixture. This fluid supposedly formed as a result of thermal impact of granitic magma on carbonate country rocks. Primary and secondary gas-liquid fluid inclusions were encountered frequently in this study, with gas present as carbon dioxide. These inclusions indicate that sapphire mineralization occurred with the participation of low-density aqueous-carbonic fluids, which carried significant concentrations of alumina. This alumina can be sufficient for sapphire crystallization.

The paragenetic sequence of the inclusions is plagioclase, diaspore, and margarite. Diaspore and margarite formed after the retrograde hydration of corundum and the plagioclase, respectively. Corundum forms through a metasomatic process of desilication. The interaction between the pegmatites and the dolomite-containing carbonates at moderate temperatures, together with the participation of aqueous-carbonic fluid, caused this desilication.

The formation of large sapphire crystals in the corundum-bearing rocks at Sutara could result from the recrystallization of early plagioclase-corundum associations when plagioclase was substituted by margarite.



Figure 17. This silver pendant contains a 65.5 ct sapphire cabochon from Sutara. Photo by Svetlana Buravleva, courtesy of A. Kurnosov.

## CONCLUSIONS

The Nezametnoye deposit is Russia's only placer deposit of jewelry-grade corundum, and the Russian jewelry market must therefore rely on sapphires and rubies from other parts of the world, most of which are treated by a variety of methods. This shortage of domestic material has prompted geologists to investigate localities previously considered unpromising. Corundum crystals were discovered in the Sutara gold mining district of the Russian Far East in 1943, but scientific studies were not carried out until recently, when the authors conducted field research in the area. We found alluvial blue, gray, bicolored pink and blue, violetish blue, and purplish pink cabochon-grade sapphires, along with corundum-bearing rocks. Sapphires—both alluvial and from corundum-bearing rocks—often feature blue and white zones. Some finished samples are more than 65 carats; most of the

crystals are heavily included with rutile needles, zircon, and biotite.

This corundum mineralization formed as the result of contact between pegmatite veins and dolomite-containing carbonate rocks, with the participation of aqueous-carbonic fluid. While only cabochon-grade

material (figures 3 and 17) was found in the Russian Far East pegmatite veins, carbonaceous rocks and products of their metamorphism with sapphire-bearing potential are widely distributed. This presents further prospects of finding new sapphire occurrences in the future.

#### ABOUT THE AUTHORS

Ms. Buravleva ([s\\_buravleva@yahoo.com](mailto:s_buravleva@yahoo.com)) is a gemologist, Dr. Pakhomova is a senior researcher in geology, and Mr. Fedoseev is an engineer at the Far East Geological Institute, Far Eastern Branch of the Russian Academy of Sciences (FEGI FEB RAS) in Vladivostok. Dr. Smirnov is senior researcher in geology at the V.S. Sobolev Institute of Geology and Mineralogy, Siberian Branch of the Russian Academy of Sciences (IGM SB RAS) in Novosibirsk.

#### ACKNOWLEDGMENTS

The authors express their gratitude to the Russian Foundation for Basic Research for financial support (grants N 13-05-90736 and 15-05-00809) and the Far Eastern Branch of the Russian Academy of Sciences (grant 14-III-B-08-172). The authors thank Mr. A. Kurnosov for permission to enter the Sutara mine.

#### REFERENCES

- Dharmaratne P.G.R., Premasiri H.M.R., Dillimuni D. (2012) Sapphires from Thammanawa, Kataragama Area, Sri Lanka. *G&G*, Vol. 48, No. 2, pp. 98–107, <http://dx.doi.org/10.5741/GEMS.48.2.98>
- Khoi N.N., Sutthirat C., Tuan D.A., Nam N.V., Thuyet N.T.M., Nhung N.T. (2011) Ruby and sapphire from the Tan Huong-Truc Lau Area, Yen Bai Province, northern Vietnam. *G&G*, Vol. 47, No. 3, pp. 182–195, <http://dx.doi.org/10.5741/GEMS.47.3.182>
- Kovrizhnykh Y.B. (1993) Corundum formations of the Russian Far East. Report on fieldwork results for corundum. *Far East Geological Department*, Vol I, pp. 34–41.
- Pakhomova V., Zhalishchak B., Tishkina V., Lapina M., Karmanov N. (2006) Mineral and melt inclusions in sapphires as an indicator of conditions of their formation and origin (Primorsky Region of the Russian Far East). *The Australian Gemmologist*, Vol. 22, No. 11, pp. 508–511.
- Pakhomova V., Buravleva S., Kurnosov A., Zhalishchak B., Tishkina V., Fedoseev D., Zharchenco S., Mouzhevsky D., Ushkova M. (2009) Corundums and Marundites of the Sutara deposit (The Russian Far East). *The Journal of the Gemmological Association of Hong Kong*, Vol. 30, pp. 47–49.
- Peretti A., Peretti F., Kanpraphai A., Bieri W.P., Hametner K., Günther D. (2008) Winza rubies identified. *Contributions to Gemology*, No. 7, Second Edition. GRS Gemresearch Swisslab, Switzerland, 97 pp.
- Peucat J.J., Ruffault P., Fritsch E., Bouhnik-Le Coz M., Simonet C., Lasnier B. (2007) Ga/Mg ratio as a new geochemical tool to differentiate magmatic from metamorphic blue sapphires. *Lithos*, Vol. 98, pp. 261–274, <http://dx.doi.org/10.1016/j.lithos.2007.05.001>
- Schmetzer K., Medenbach O. (1988) Examination of three-phase inclusions in colorless, yellow, and blue sapphires from Sri Lanka. *G&G*, Vol. 24, No. 2, pp. 107–111, <http://dx.doi.org/10.5741/GEMS.24.2.107>
- Schwarz D., Pardieu V., Saul J.M., Schmetzer K., Laurs B.M., Giuliani G., Klemm L., Malsy A.-K., Erel E., Hauzenberger C., Du Toit G., Fallick A.E., Ohnenstetter D. (2008) Rubies and sapphires from Winza, Central Tanzania. *G&G*, Vol. 44, No. 4, pp. 322–347, <http://dx.doi.org/10.5741/GEMS.44.4.322>
- Shaposhnikov E.Y. (1945) Corundum mineralization of the Sutara mine. Report on fieldwork results for corundum in 1943 and 1944 in the Sutara Mine district (Birsky Region of the Jewish Autonomous District of the Khabarovsk Krai). *Far East Geological Department*, 103 pp.
- Shor R., Weldon R. (2009) Ruby and sapphire production and distribution: A quarter century of change. *G&G*, Vol. 45, No. 4, pp. 236–259, <http://dx.doi.org/10.5741/GEMS.45.4.236>
- Vaskin A.F. (1999) State geological map of the Russian Federation. 1: 200 000, VSEGEL, St. Petersburg, 196 pp.